One dimensional models for blood flow in arteries[*]

Luca Formaggia[a], Daniele Lamponi[a], Alfio Quarteroni[a,b]

[a] Institut de Mathématiques (FSB/IMA), Ecole Polytecnique Fédérale de Lausanne
CH-1015 Lausanne, Switzerland

[b] MOX, Dipartimento di Matematica, Politecnico di Milano
P.zza Leonardo da Vinci 32, 20133 Milano, Italy

July 2002

Abstract

We investigate a family of one dimensional nonlinear systems which model the blood pulse propagation in compliant arteries. They are obtained by averaging the Navier-Stokes equation on each section of an arterial vessel and using simplified models for the vessel compliance. Different differential operators arise depending on the simplifications made on the structural model. Starting from the most basic assumption of pure elastic instantaneous equilibrium, which provides a well known algebraic relation between intramural pressure and vessel section area, we analyse in turn the effects of terms accounting for inertia, longitudinal pre-stress and viscoelasticity.

We also consider the problem of how to account for branching and possible discontinuous wall properties, the latter aspect is relevant in the presence of prosthesis and stents. To this purpose we employ a domain decomposition approach and we provide conditions which ensure the stability of the coupling.

We propose a numerical method based on a finite element Taylor-Galerkin scheme combined with operator splitting techniques, and carry out several test cases for the assessment of the proposed models.

1   Introduction

In this work we will introduce one dimensional models [18, 17, 24] to compute the blood flow and pressure wave propagation in the human arterial system. These models can be used as an alternative to the more complex three dimensional fluid-structure models or in conjunction with them in a geometrical multiscale fashion, as explained in [9]. Their computational complexity is several orders of magnitude lower than that of multidimensional models based on the coupling of the Navier-Stokes equations for the flow field in the arterial lumen and a mechanical model for the vessel wall displacement, at the price of providing just averaged information.

However, they give a good description of the propagation of pressure waves in arteries [33, 19], hence they can be successfully used to investigate the effects on pulse waves of the geometrical and mechanical arterial modification, due e.g. to the presence of stenoses, or to the placement of stents or prostheses [8, 35, 29]. Their low computational cost makes it possible not only to study pressure wave propagation on isolated arterial segment, like in [21, 22, 15, 16], but also the global circulation [30, 14, 15] system, here represented by a network of one-dimensional models.

In the framework of a multiscale approach, one dimensional models may be coupled on one hand with lumped parameter models [9, 25] based on system of ordinary differential equations [28, 36] or, on the other hand, to three dimensional fluid-structure models, as discussed in [6] and in [7]. In the latter case they may also provide a way of implementing more realistic boundary conditions for 3D calculations. Or, they can be used for the numerical acceleration of a three dimensional Navier-Stokes solver in a multilevel-multiscale scheme [5].

---

[*] Submitted to *Journal of Engineering Mathematics*

In this paper we first recall the basic 1D model for a single artery approximated as a straight cylinder. This model is represented by a system of two partial differential equations describing the evolution of the section area A and the mass flux Q along the vessel axis, and, as a consequence, that of the mean pressure p.

The mean pressure is indeed liked to A by a relation derived by the mechanics of the vessel wall structure. In this paper we will consider two possibilities (among the various presented in the literature, see e.g. [24, 21]). The first choice corresponds to assuming an instantaneous static equilibrium for the vessel wall and leads to a hyperbolic system of equations of the type already discussed and analysed in [9, 6, 8] and [24]. In this work we will recall the main results and further develop the method adopted for the numerical approximation.

When we account for inertia or other mechanical properties such viscoelasticity or longitudinal pre-stress, the relation between pressure and vessel area is given by a differential equation. However, it is still possible, at a price of some simplifications in the model, to recover a system of two partial differential equations for the vessel section area A and the flux Q, as already illustrated in [9]. By doing so, it may be easily recognised that the wall inertia introduces an additional dispersive term, while viscoelasticity contributes with a diffusive operator. Here, we treat these additional terms by an operator splitting technique and carry out numerical tests to exemplify their effect on the pressure and flow pattern and to understand their relevance for practical application. It has been found that for physiological situations inertia and viscoelastic effects are practically negligible, while accounting for longitudinal pre-stress may have a marked regularising effect when there are abrupt variations in the mechanical characteristics of the vessel walls.

As a consequence of some vascular pathologies, a tract of an artery has either to be replaced by a prosthesis or reinforced by the application of a stent (a metallic wire-mesh). In both cases the elastic properties of the vessel changes abruptly. The problem may be treated by regularising the transition region between the healthy artery and the prosthesis, as described in [8]. Here we investigate an alternative approach based on domain decomposition (DD) methods. However, for the problem at hand the interface conditions which might be imposed at the interface is not unique. We will present several alternatives, justified by physical arguments, and we will show how for a particular choice it is possible to obtain an energy inequality for the coupled system.

The human arterial system is formed by a network of vessels: even if we approximate each arterial segment by using a one-dimensional description, we need to find a proper way to account for branching. A DD technique has been developed also to treat this situation.

The paper layout is as follows. In section 2 we recall the basic 1D nonlinear hyperbolic model for a single cylindrical straight arterial element. Then we illustrate the Taylor-Galerkin scheme that we use for the numerical approximation, and analyse how to impose the conditions (physical and numerical) that need to be provided at the proximal and distal boundaries. In section 3 we present a domain decomposition strategy applied to the simulation of a stent implant and branching. Interface conditions, which satisfy an energy inequality, are proposed and the problem of bifurcation with specific angles is treated. In section 4 we consider more complex vessel law by adding inertia, viscoelastic, longitudinal pre-stress terms at the basic algebraic law. We present a numerical framework where these additional terms are treated by an operator splitting approach. Finally we present several numerical results.

2   The derivation of the basic one dimensional model

One dimensional models provide a simplified description of the flow motion in arteries and its interaction with the vessel wall displacement. Although being inappropriate to provide details on the flow field (such as recirculation or oscillating shear stresses), they can however effectively describe the propagative phenomena due to the wall compliance. They are derived from the Navier Stokes equations

$$\begin{cases} \dfrac{\partial \mathbf{u}}{\partial t} + (\mathbf{u} \cdot \nabla)\,\mathbf{u} + \dfrac{1}{\rho}\nabla P - \text{div}\left[\nu(\nabla\mathbf{u} + (\nabla\mathbf{u})^T)\right] = 0 \\ \text{div } \mathbf{u} = 0 \end{cases} \tag{1}$$

posed on a cylindrical domain Ω_t which changes in time because of the flow induced wall movement. Here $\mathbf{u} = (u_x, u_y, u_z)$ is the fluid velocity, P the pressure, ν the kinematic viscosity and ρ the blood density; (x, y, z) is a system of Cartesian coordinates.
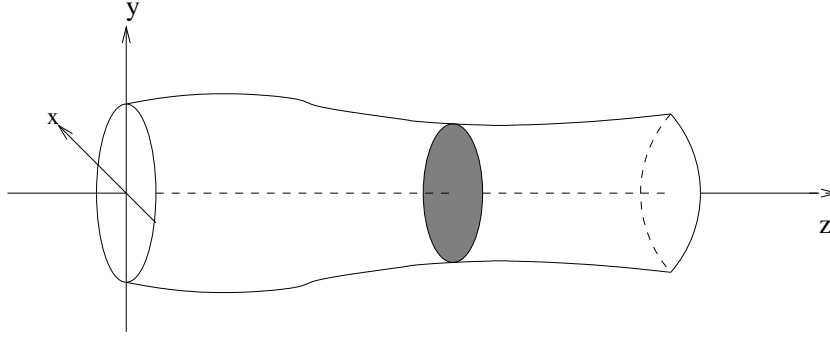
Figure 1: The cylindrical domain Ω_t. The cylinder axis is aligned with the coordinate z. The axial sections $z =$const. remain circular at all times.

A straightforward derivation of one dimensional models can be found in [24] and is not repeated here. We just recall the main assumptions behind this derivation.

The domain, Ω_t, is a straight cylinder (with axis oriented along the coordinate z), as depicted in Fig. 1. It is comprised between $z = 0$ and $z = L$, L being the vessel length, which is assumed time invariant. We will also employ cylindrical coordinates, denoted by (r, θ, z). We make the assumption of axial symmetry for all the quantities involved. Furthermore a wall displacement along the radial direction is considered. This has the implication that each axial section S remains circular at all times, i.e., for $z \in [0, L]$ and $t > 0$ we have

$$S = S(z, t) = \{(r, \theta, z) : 0 \leq r \leq R(z, t), 0 \leq \theta < 2\pi\},$$

where $R = R(z, t)$ is the vessel radius. The pressure is taken to be constant on each axial section and we assume that viscous effects are relevant only near the wall boundary. The component u_z is dominant with respect to u_x and u_y and furthermore we assume that it may be described in cylindrical coordinates as

$$u_z(r, z, t) = \overline{u}(z, t) s \left(\frac{r}{R(z, t)} \right),$$

where $\overline{u}$ is the mean velocity on each axial section and $s : \mathbb{R} \to \mathbb{R}$ is a velocity profile (also called *profile law*).

The vessel wall is supposed to be impermeable (although seepage of fluid through the wall may be accounted at the expense of a slight modification of the equations). By integrating (1) over a generic axial section $S(z, t)$ and taking advantage of the above assumptions, one obtains the following system

$$\frac{\partial A}{\partial t} + \frac{\partial Q}{\partial z} = 0 \tag{2}$$

$$\frac{\partial Q}{\partial t} + \frac{\partial}{\partial z} \left(\alpha \frac{Q^2}{A} \right) + \frac{A}{\rho} \frac{\partial P}{\partial z} + K_R \frac{Q}{A} = 0 \tag{3}$$

for all $z \in (0, L)$ and $t > 0$, where the unknowns A, Q and P (in the following we will also use the notation $p = \frac{P}{\rho}$) denote the section area, averaged volume flux and mean pressure, respectively, and they are defined as

$$A(z, t) = \int_{S(z,t)} dz, \quad Q(z, t) = \int_{S(z,t)} u_z(x, y, z, t) dx\, dy,$$
$$P(z, t) = (A(z, t))^{-1} \int_{S(z,t)} P(x, y, z, t) dx\, dy \tag{4}$$

Note that $Q = A\overline{u}$. The coefficient α is the momentum correction coefficient (also called Coriolis coefficient), defined as

$$\alpha = \frac{\int_S u_z^2 d\gamma}{A\overline{u}^2} = \frac{\int_S s^2 \, d\gamma}{A},$$

3

while K_R is a resistance parameter related to the viscosity of blood. For a profile law of the form

$$s(x) = \zeta^{-1}(\zeta + 2)(1 - x^{\zeta}),$$

with $\zeta > 0$, we have $\alpha = (\zeta + 2)(\zeta + 1)^{-1}$. In particular, for a parabolic profile (Poiseuille flow) one has $\zeta = 2$ and hence $\alpha = \frac{4}{3}$. In blood flow problems a flatter profile ($\zeta = 9$) is more in accordance with experimental findings. For instance, in [31] the value $\alpha = 1.1$ is suggested. Also the choice $\alpha = 1$ is often used since it leads to considerable mathematical simplifications. As for the resistance parameter, a parabolic profile would provide $K_R = 8\pi\nu$, which is the value normally used.

To close our problem it is necessary to provide an additional relation. This is usually derived from a mechanical model for the vessel wall displacement. Here we have considered the generalised string model [25], which is written in the following form

$$\rho_w h_0 \frac{\partial^2 \eta}{\partial t^2} - \tilde{\gamma}\frac{\partial \eta}{\partial t} - \tilde{a}\frac{\partial^2 \eta}{\partial z^2} - \tilde{c}\frac{\partial^3 \eta}{\partial t \partial z^2} + \tilde{b}\eta = (P - P_{ext}), \quad z \in (0, L), \, t > 0. \tag{5}$$

Here $\eta = R - R_0$ is the displacement of the vessel wall with respect to a reference configuration, at the initial time t=0:

$$\Omega_0 = \{(r, \theta, z) : 0 \le r \le R_0(z), \, 0 \le \theta < 2\pi, \, 0 \le z \le L\}$$

which corresponds to that taken by the vessel when filled by a still fluid a pressure equal to the external pressure P_{ext} (here taken constant).

We may identify the physical significance of the various terms. The first one is the inertia term, proportional to the acceleration of the vessel wall. The second term is a Voigt-type, viscoelastic term, proportional to the radial displacement velocity. The third term is related to the longitudinal pre-stress state of the vessel. It is indeed well known that in physiological conditions an artery is subjected to a longitudinal tension. The fourth term is an another viscoelastic term while the last term is the elastic response function.

We have

$$\eta = \frac{\sqrt{A} - \sqrt{A_0}}{\sqrt{\pi}}, \quad \text{with } A_0 = \pi R_0^2. \tag{6}$$

ρ_w is the vessel density, h_0 the wall thickness at the reference configuration, $\tilde{a}, \tilde{b}$ and $\tilde{c}$ three positive coefficients. In particular,

$$\tilde{b} = \frac{Eh_0}{\kappa R_0^2} = \frac{\pi E h_0}{\kappa A_0}, \tag{7}$$

where E is the Young modulus of elasticity and κ may take the value 1 or $3/4$ depending whether the assumption of uni-axial of plane stresses is made in the derivation of the generalised string model. More details are found in the cited reference. In this work, we have taken $\kappa = 1$.

The partial differential equation (5) may be used to link the pressure with the vessel area and its time and spatial derivatives. However, its direct use in the context of our one dimensional model is rather problematic. The system formed by (2), (3) and (5) (after having expressed the latter in terms of A by using (6)) would contain two evolution equations for the same unknowns, the area A.

$$\frac{\partial A}{\partial t} + \frac{\partial Q}{\partial z} = 0$$

$$\frac{\partial Q}{\partial t} + \frac{\partial}{\partial z}\left(\alpha\frac{Q^2}{A}\right) + \frac{A}{\rho}\frac{\partial P}{\partial z} + K_R\frac{Q}{A} = 0 \tag{8}$$

$$\rho_w h_0 \frac{\partial^2 \eta}{\partial t^2} - \tilde{\gamma}\frac{\partial \eta}{\partial t} - \tilde{a}\frac{\partial^2 \eta}{\partial z^2} - \tilde{c}\frac{\partial^3 \eta}{\partial t \partial z^2} + \tilde{b}\eta = (P - P_{ext})$$

Moreover, it is known that for the problem at hand the elastic response is the dominating effect, while the other terms are less important. Consequently, a first model is obtained by neglecting all derivatives in (5). Pressure and area will then be related by an algebraic law of the type

$$P - P_{ext} = \tilde{b}\eta = \beta\frac{\sqrt{A} - \sqrt{A_0}}{A_0} \tag{9}$$

4

where

$$\beta = E h_0 \sqrt{\pi} \tag{10}$$

is in general a function of z trough the Young modulus E.

In a more general setting, the algebraic relationship may be expressed as

$$P = P_{ext} + \psi(A; A_0, \beta) \tag{11}$$

where we have outlined that the pressure will also depend parametrically on A_0 and on a set of coefficients $\beta = \{\beta_1, \beta_2, ...\beta_n\}$ which account for physical and mechanical characteristics of the vessel. Both A_0 and β are given functions of z, while it is assumed that they do not vary in time. It is required that ψ be (at least) a C^1 function of its arguments and be defined for all positive values of A and A_0, whereas the range of variation of β will depend on the particular mechanical model chosen. In addition we must have, for all allowable values of A, A_0 and β, that

$$\frac{\partial \psi}{\partial A} > 0, \quad \text{and that} \quad \psi(A_0; A_0, \beta) = 0.$$

Various algebraic relations of the form (11) may be found in the literature for one dimensional models of blood flow. The interested reader may refer, for instance, to [24] and the references therein. In this work we will adopt the relation (9), i.e. $\psi = \beta \frac{\sqrt{A} - \sqrt{A_0}}{A_0}$, and β reduces to a single parameter $\beta = \beta_1$. Furthermore, for the sake of simplicity, and without loss of generality, we will assume $P_{ext} = 0$. We also introduce the quantity

$$c_1 = \sqrt{\frac{A}{\rho} \frac{\partial \psi}{\partial A}}, \tag{12}$$

which in our case may be readily computed as

$$c_1 = \sqrt{\frac{\beta}{2\rho A_0}} A^{\frac{1}{4}}.$$

We will now focus on the differential problem obtained by substituting (9) into (3), and on its numerical solution, leaving to a later section a discussion on how to implement the other terms in (5) into the model.

2.1 One dimensional model with algebraic pressure law

By replacing (9) into (3), after some simple manipulations we obtain a system of differential equations for the evolution of A and Q which may be written in conservation form as

$$\frac{\partial \mathbf{U}}{\partial t} + \frac{\partial \mathbf{F}}{\partial z}(\mathbf{U}) = \mathbf{B}(\mathbf{U}), \quad z \in (0, L), \quad t > 0 \tag{13}$$

where $\mathbf{U} = [A, Q]^T$ are the conservative variables, $\mathbf{F} = [F_A, F_Q]^T$ the corresponding fluxes and $\mathbf{B} = [B_A, B_Q]^T$ a source term. Details may be found in [24]. More precisely, by choosing (9) we obtain

$$\mathbf{F}(\mathbf{U}) = \begin{bmatrix} Q \\ \alpha \dfrac{Q^2}{A} + \displaystyle\int_0^A c_1^2 \, dA \end{bmatrix} = \begin{bmatrix} Q \\ \alpha \dfrac{Q^2}{A} + \dfrac{\beta}{3\rho A_0} A^{\frac{3}{2}} \end{bmatrix} \tag{14}$$

$$\mathbf{B}(\mathbf{U}) = \begin{bmatrix} 0 \\ K_R \dfrac{Q}{A} + \dfrac{A}{A_0 \rho}\left(\dfrac{2}{3} A^{\frac{1}{2}} - A_0^{\frac{1}{2}}\right) \dfrac{\partial \beta}{\partial z} \\ \quad - \dfrac{\beta}{\rho} \dfrac{A}{A_0^2}\left(\dfrac{2}{3} A^{\frac{1}{2}} - \dfrac{1}{2} A_0^{\frac{1}{2}}\right) \dfrac{\partial A_0}{\partial z} \end{bmatrix}. \tag{15}$$

Both the spatial variation of the reference area A_0 and that of the Young's modulus β contribute to the source term. We also point out that the derivation of the conservative form may be carried out if β and A_0 are smooth functions of z. The flux Jacobian $\mathbf{H}$ may be readily computed as

$$\mathbf{H}(\mathbf{U}) \quad = \quad \frac{\partial \mathbf{F}}{\partial \mathbf{U}} = \left[\begin{array}{cc} 0 & 1 \\ -\alpha\dfrac{Q^2}{A^2} + \dfrac{\beta}{2\rho A_0}A^{\frac{1}{2}} & 2\alpha\dfrac{Q}{A} \end{array} \right]. \tag{16}$$

The characteristic analysis, whose details may be found in [24], shows that for all allowable $\mathbf{U}$ (that is for $A > 0$) the system is strictly hyperbolic and the eigenvalues of $\mathbf{H}$ are

$$\lambda_{1,2} \quad = \quad \alpha\frac{Q}{A} \pm \sqrt{c_1^2 + \alpha(\alpha-1)\frac{Q^2}{A^2}}. \tag{17}$$

Where $\alpha = 1$ the computation of global characteristic variables $\mathbf{W}(\mathbf{U}) = [W_1(\mathbf{U}), W_2(\mathbf{U})]^T$ is straightforward and yields

$$W_{1,2} = \frac{Q}{A} \pm 4\sqrt{\frac{\beta}{2\rho A_0}}A^{\frac{1}{4}}, \tag{18}$$

see [24]. These relations can be inverted to express the primitive variables in terms of the characteristic ones,

$$A = \left(\frac{2\rho A_0}{\beta}\right)^2 \left(\frac{W_1 - W_2}{8}\right)^4, \qquad Q = A\frac{W_1 + W_2}{2}, \tag{19}$$

allowing, in particular, the implementation of boundary and compatibility conditions, as will be briefly discussed later.

2.2 Numerical Discretisation

We discretize system (13) by a second order Taylor-Galerkin scheme [3]. The derivation here is made sightly more involved than for the classical systems of conservation laws due to the presence of the source term.

From (13) we may write

$$\frac{\partial \mathbf{U}}{\partial t} = \mathbf{B} - \frac{\partial \mathbf{F}}{\partial z} \tag{20}$$

$$\frac{\partial^2 \mathbf{U}}{\partial t^2} = \mathbf{B_U}\frac{\partial \mathbf{U}}{\partial t} - \frac{\partial}{\partial z}\left(\mathbf{H}\frac{\partial \mathbf{U}}{\partial t}\right) = \mathbf{B_U}\left(\mathbf{B} - \frac{\partial \mathbf{F}}{\partial z}\right) - \frac{\partial(\mathbf{HB})}{\partial z} + \frac{\partial}{\partial z}\left(\mathbf{H}\frac{\partial \mathbf{F}}{\partial z}\right), \tag{21}$$

where we have denoted $\mathbf{B_U} = \dfrac{\partial \mathbf{B}}{\partial \mathbf{U}}$. We now consider the time intervals (t^n, t^{n+1}), for $n = 0, 1, \ldots$, with $t^n = n\Delta t$, Δt being the time step, and we discretize in time using a Taylor series truncated at the second order, to obtain the following semi-discrete system for the approximation $\mathbf{U}^n$ of $\mathbf{U}(t^n)$

$$\mathbf{U}^{n+1} \quad = \quad \mathbf{U}^n - \Delta t\frac{\partial}{\partial z}\left[\mathbf{F}^n + \frac{\Delta t}{2}\mathbf{H}^n\mathbf{B}^n\right] - \frac{\Delta t^2}{2}\left[\mathbf{B}_\mathbf{U}^n\frac{\partial \mathbf{F}^n}{\partial z} - \frac{\partial}{\partial z}\left(\mathbf{H}^n\frac{\partial \mathbf{F}^n}{\partial z}\right)\right]$$
$$+ \Delta t\left(\mathbf{B}^n + \frac{\Delta t}{2}\mathbf{B}_\mathbf{U}^n\mathbf{B}^n\right), \quad n = 0, 1, \ldots, \tag{22}$$

where $\mathbf{U}^0$ is provided by the initial conditions and $\mathbf{F}^n$ stands for $\mathbf{F}(\mathbf{U}^n)$ (a similar notation holds for $\mathbf{H}^n$, $\mathbf{B}^n$ and $\mathbf{B}_\mathbf{U}^n$).

The space discretisation is carried out using the Galerkin finite elements method. The interval $[0, L]$ is subdivided into N elements $[z_i, z_{i+1}]$, with $i = 0, \ldots, N$ and $z_{i+1} = z_i + h_i$, with $\sum_{i=0}^{N-1} h_i = L$, where h_i is the local element size. Let V_h be the space of piecewise linear finite element functions and $\mathbf{V}_h = [V_h]^2$, while $\mathbf{V_h^0} = \{\mathbf{v}_h \in \mathbf{V}_h \,|\, \mathbf{v}_h = \mathbf{0} \text{ at } z = 0 \text{ and } z = L\}$. Further, we indicate by

$$(\mathbf{u}, \mathbf{v}) = \int_0^L \mathbf{u} \cdot \mathbf{v}dz$$

6

the $\mathbf{L}^2(0, L)$ scalar product.

Using the abridged notations

$$\mathbf{F}_{LW}(\mathbf{U}) = \mathbf{F}(\mathbf{U}) + \frac{\Delta t}{2}\mathbf{H}(\mathbf{U})\mathbf{B}(\mathbf{U})$$

and

$$\mathbf{B}_{LW}(\mathbf{U}) = \mathbf{B}(\mathbf{U}) + \frac{\Delta t}{2}\mathbf{B}_{\mathbf{U}}(\mathbf{U})\mathbf{B}(\mathbf{U}),$$

the finite element formulation of (22) is :

for $n \geq 0$, find $\mathbf{U}_h^{n+1} \in \mathbf{V}_h$ which satisfies the following "interior" equations

$$
\begin{aligned}
(\mathbf{U}_h^{n+1}, \psi_h) &= (\mathbf{U}_h^n, \psi_h) + \Delta t \left(\mathbf{F}_{LW}(\mathbf{U}_h^n), \frac{d\psi_h}{dz}\right) - \frac{\Delta t^2}{2}\left(\mathbf{B}_{\mathbf{U}}(\mathbf{U}_h^n)\frac{\partial \mathbf{F}(\mathbf{U}_h^n)}{\partial z}, \psi_h\right) \\
&\quad - \frac{\Delta t^2}{2}\left(\mathbf{H}(\mathbf{U}_h^n)\frac{\partial \mathbf{F}}{\partial z}(\mathbf{U}_h^n), \frac{d\psi_h}{dz}\right) + \Delta t \left(\mathbf{B}_{LW}(\mathbf{U}_h^n), \psi_h\right), \ \forall \psi_h \in \mathbf{V}_h^0
\end{aligned}
\tag{23}
$$

together with the boundary and compatibility conditions to be discussed in the next section.

A third-order scheme (in time) may be derived following the indications in [1]. However, in our case this would imply the coupling of the equations for A_h and Q_h, that are completely decoupled in (23) . For this reason, we have considered only the second-order scheme. However, many of the considerations that we develop in this note will apply also to the third-order version.

The second order Taylor-Galerkin scheme (23) entails a time step limitation. A linear stability analysis [23] indicates that the following condition should be satisfied

$$\Delta t \leq \frac{\sqrt{3}}{3} \min_{0 \leq i \leq N}\left[\frac{h_i}{\max(\lambda_{1,i}, \lambda_{1,i+1})}\right], \tag{24}$$

where $\lambda_{1,i}$ here indicates the value of λ_1 at mesh node z_i. This condition corresponds to a CFL number of $\frac{\sqrt{3}}{3}$, typical of a second order Taylor-Galerkin scheme in one dimension [23].

2.3   Boundary and compatibility conditions

For the flow regimes we are interested in, the two eigenvalues λ_1 and λ_2 have opposite sign, hence the differential problem needs exactly one boundary condition at $z = 0$ and one at $z = L$. Whenever an explicit formulation of the characteristic variables is available, boundary conditions may be expressed directly in terms of the entering characteristic variable. For instance, at the boundary $z = 0$, an admissible boundary condition is

$$W_1(t) = g_1(t), \quad \text{at } z = 0, \, t > 0, \tag{25}$$

g_1 being a given function. If we do not have an explicit expression for the characteristic variables, we might use instead the pseudo-characteristic approach (see e.g. [26]).

However, (25) is seldom applied directly as the available data is usually given in terms of the physical variables. For instance, at the inlet (or proximal section) we may wish to impose the pressure or the mass flux (maybe obtained from measurements). The issue of admissibility of a boundary condition for a general non-linear hyperbolic system has been addressed in [4], other references may be found in [11]. In our specific case, the imposition of average pressure at the inlet $z = 0$ is admissible.

At the outlet or, better said, distal section, in absence of a specific information on pressure or flux variation, an important class of boundary conditions, called non-reflecting, are those that allow the simple wave solution associated to the outgoing characteristic to leave the domain. Following [34] they may be written as

$$\mathbf{l}_2^T \left(\frac{\partial \mathbf{U}}{\partial t} - \mathbf{B}(\mathbf{U})\right) = 0, \quad z = L, \, t > 0 \tag{26}$$

7

for all $t > 0$. Here, $\mathbf{l}_1$ and $\mathbf{l}_2$ are the left eigenvectors associated to λ_1 and λ_2, respectively. When $\mathbf{B}(\mathbf{U}) = \mathbf{0}$ they are equivalent to impose a constant value (typically set to zero) to the incoming characteristic variable. When $\mathbf{B} = \mathbf{0}$ they account for the variation of the characteristic variables due to the presence of the source term.

Although the differential problem requires only one (physical) boundary condition at each end of the tube, the solution of the numerical problem requires to prescribe a full set of values for A and Q at the first and last node. We need two extra relations, which are provided by the differential equations 'projected' along the direction of the outgoing characteristics, i.e.

$$\mathbf{l}_2^T \left(\frac{\partial \mathbf{U}}{\partial t} + \frac{\partial \mathbf{F}}{\partial z}(\mathbf{U}) - \mathbf{B}(\mathbf{U}) \right) = 0, \qquad z = 0,\, t > 0$$

$$\mathbf{l}_1^T \left(\frac{\partial \mathbf{U}}{\partial t} + \frac{\partial \mathbf{F}}{\partial z}(\mathbf{U}) - \mathbf{B}(\mathbf{U}) \right) = 0, \quad z = L,\, t > 0. \tag{27}$$

These compatibility relations could be discretized by adopting the same basic scheme as the differential problem. However, this would result in relations that couple the values of A_h^{n+1} and Q_h^{n+1} at the vessel ends. Since it is preferable for computational reasons to maintain two decoupled discrete systems for the evolution of area and mass flow, we have here resorted to a different set of compatibility relations called "characteristic extrapolation". It is based on the well known fact that the characteristic variables satisfy a system of ordinary differential equations along the characteristic path. Indeed, when $\mathbf{B}(\mathbf{U}) = 0$ the characteristic variables are constant along the characteristics, so a first order approximation of the outgoing characteristic variables at time t^{n+1} and $z = 0$ and $z = L$, respectively, is provided by

$$W_2^{n+1}(0) = W_2^n(-\lambda_2^n(0)\Delta t), \quad W_1^{n+1}(L) = W_1^n(L - \lambda_1^n(L)\Delta t).$$

A second order approximation might be obtained by following the technique described in [2]. When $\mathbf{B}(\mathbf{U}) \neq 0$ the values of $W_2^{n+1}(0)$ and $W_1^{n+1}(L)$ will have to be computed by numerically solving the associated ODE system. The value of $W_2^{n+1}(0)$ and $W_1^{n+1}(L)$ together with the boundary conditions effectively complements the discrete system provided by (23). Again, if the characteristic variables are not available the pseudo-characteristics may be used instead. Since from now on we assume $\alpha = 1$, the characteristic variables are given by (18).

3   Domain decomposition approach for prosthesis and bifurcations

When a stent or a prosthesis such as the one depicted in Fig. 2 is implanted to alleviate severe vascular pathologies, it causes an abrupt variation of the elastic properties along the artery. In principle this could be taken into account by allowing β to have a discontinuity at the interfaces between the "healthy" and the prosthetic artery, while being a smooth function otherwise. Here we will first consider the case of a single discontinuity at $z = \Gamma \in (0, L)$. By following the arguments in [35] we may derive that in this situation A (and consequently p) is (in general) discontinuous at $z = \Gamma$ and, consequently, the product $A\frac{\partial p}{\partial z}$ in equation (3) is not well defined at this location.

A possibility to overcome this problem is to perform a regularisation of β, as done in [8]. However, this requires the use of a fine mesh around Γ to properly represent the transition, with a consequent loss of efficiency of the numerical scheme because of condition (24). Furthermore, if the solution is very steep, the Taylor-Galerkin scheme should be stabilised to avoid spurious oscillations, with the inevitable addition of extra numerical dissipation.

We will here investigate instead an alternative solution provided by the domain decomposition approach (see [27]). In Fig. 3 we show the vessel Ω partitioned into two subdomains $\Omega_1 = (0, \Gamma)$ and $\Omega_2 = (\Gamma, L)$. For a standard system in conservation form, the interface condition would entail the continuity of the fluxes, which corresponds to the Rankine-Huguenot condition for a discontinuity that does not propagate. Unfortunately, in view of the previous considerations, it is arguable whether the interface conditions can be derived from the equations in form (13) since they have been obtained under the requirement that the solution be smooth. Clearly, the problem concerns only the momentum equation as the continuity equation is originally in conservation form and, by standard arguments, this yields mass flux continuity across the interface (a fact that agrees with the physical intuition):

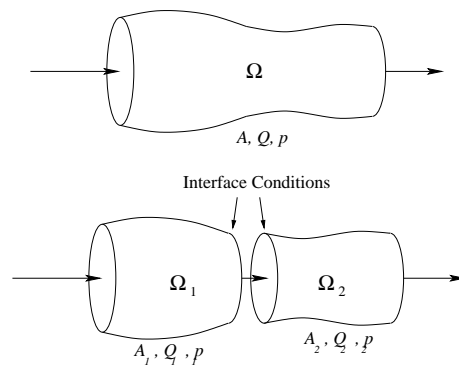$$[Q] = Q|_{\Gamma+} - Q|_{\Gamma-} = 0. \tag{28}$$

8

Figure 2: Endograft

Figure 3: Domain decomposition of an artery featuring a discontinuous Young modulus

The jump condition for the momentum equation has to be driven instead by other considerations. A possibility, investigated in [35], is to consider the limit of a regularised problem. Yet, this procedure is not completely satisfactory, since the limit will in general depend on the way the regularisation procedure is carried out. Another possibility often encountered in the literature for similar situations [15] is to impose the continuity of pressure. Yet, this condition would imply a possible increase of the energy of the system through the discontinuity, a condition hardly justifiable by physical means. Here we have followed the route of searching for a condition which would guarantee an energy inequality for the coupled problem.

In Lemma 2.1 of [6] it has been shown that our problem, in the case of $\alpha = 1$, satisfies the following energy inequality

$$\varepsilon(t) + K_R \int_0^t \int_0^L \bar{u}^2 dz dt + \int_0^t [Q p_t]_0^L \, dt \leq \varepsilon(0) \tag{29}$$

where

$$\varepsilon(t) = \int_0^L (\frac{1}{2} A(z,t) \bar{u}^2(z,t) + \frac{1}{\rho} \int_{A_0}^{A(z,t)} \psi(\zeta) d\zeta) dz,$$

while $p_t = p + \frac{1}{2} \bar{u}^2$ is the total pressure and $[f]_0^L = f(L) - f(0)$.

In the domain decomposition case of Fig. (3), indicating quantities in Ω_i with the subscript $i = 1, 2$, we obtain, by summing inequality (29) applied to the problem in each subdomain,

$$\varepsilon_1(t) + K_R \int_0^t \int_0^\Gamma \bar{u}_1^2 dz dt + \varepsilon_2(t) + K_R \int_0^t \int_\Gamma^L \bar{u}_2^2 dz dt + \int_0^t (Q_2 p_{t,2}|_L - Q_1 p_{t,1}|_0) dt +$$
$$\int_0^t (Q_1 p_{t,1} - Q_2 p_{t,2})|_\Gamma dt \leq \varepsilon_1(0) + \varepsilon_2(0), \quad t > 0. \tag{30}$$

Should we require that

$$Q_1 p_{t,1} \geq Q_2 p_{t,2} \tag{31}$$

at the interface point Γ we would obtain an energy inequality equivalent to that of the single domain case. Then, by imposing suitable restrictions on the boundary data following the same arguments given in [6], we obtain a global energy estimate in the form

$$\varepsilon_1(t) + \varepsilon_2(t) + K_R \left[\int_0^t \left(\int_0^\Gamma \bar{u}_1^2 dz + \int_\Gamma^L \bar{u}_2^2 dz \right) dt \right] \leq \varepsilon_1(0) + \varepsilon_2(0) + \xi(t) \tag{32}$$

where ξ is a quantity which depends only on the boundary data and on t. Thanks to (28) condition (31) is in particular satisfied by the choice $p_{t,1} = p_{t,2}$; in view of this results we have chosen the following interface conditions

$$\begin{cases} Q_1 = Q_2 \\ p_{t,1} = p_{t,2} \end{cases} \quad \text{on } z = \Gamma, \quad t > 0. \tag{33}$$

Therefore the coupled problem reads, in each domain $\Omega_i, i = 1, 2$.

$$\begin{cases} \dfrac{\partial A_i}{\partial t} + \dfrac{\partial Q_i}{\partial z} = 0 \\ \dfrac{\partial Q_i}{\partial t} + \dfrac{\partial}{\partial z} \left(\dfrac{Q_i^2}{A_i} \right) + A_i \dfrac{\partial p_i}{\partial z} + K_R \dfrac{Q_i}{A_i} = 0 \end{cases} , t > 0, \tag{34}$$

together with the interface condition (33) and appropriate boundary conditions at $z = 0$ and $z = L$.

To solve the problems in Ω_1 and Ω_2 separately, we have devised a decoupling technique which, at each time step from t^n to t^{n+1}, provides the Taylor-Galerkin algorithm with the values Q_i^{n+1} and A_i^{n+1} of the unknowns at the interface Γ, for $i = 1, 2$. We need to use (33) together with the compatibility conditions, for instance in the form of the extrapolation of the characteristic variables exiting Ω_1 and Ω_2 at Γ. We indicate with $W_{1,1}^{n+1}$ and $W_{2,2}^{n+1}$ the values at $z = \Gamma$ and $t = t^{n+1}$ of the (outgoing) characteristic variables W_1 and W_2, relative to domain Ω_1

10

and Ω_2, respectively, obtained by extrapolation from the data at $t = t^n$. Using relation (18) we finally obtain a non linear system for the interface variable, namely

$$
\begin{cases}
Q_1^{n+1} - Q_2^{n+1} = 0 \\
\psi(A_1^{n+1}; A_{0,1}, \beta_1) + \left(\dfrac{Q_1^{n+1}}{A_1^{n+1}}\right)^2 - \psi(A_2^{n+1}; A_{0,2}, \beta_2) + \left(\dfrac{Q_2^{n+1}}{A_2^{n+1}}\right)^2 = 0 \\
\dfrac{Q_1^{n+1}}{A_1^{n+1}} + 4\sqrt{\dfrac{\beta_1}{2\rho A_{0,1}}}\left(A_1^{n+1}\right)^{\frac{1}{4}} - W_{1,1}^{n+1} = 0 \\
\dfrac{Q_2^{n+1}}{A_2^{n+1}} - 4\sqrt{\dfrac{\beta_2}{2\rho A_{0,2}}}\left(A_2^{n+1}\right)^{\frac{1}{4}} - W_{2,2}^{n+1} = 0
\end{cases}
\qquad \text{at } z = \Gamma \qquad (35)
$$

which is solved by a Newton iteration. Here, β_i and $A_{0,i}$ indicate the values of β and A_0 in Ω_i and, for the sake of generality, we have assumed that the reference section area A_0 might be discontinuous at $z = \Gamma$. It has been verified that the determinant of the Jacobian of system (35) is different from zero for all allowable values of the parameters, thus guaranteeing that the Newton iteration is well-posed. It has also been found that, by using as starting values the unknowns at time t^n, the method converges in few iterations with a tolerance of 10^{-8} on the relative increment.

For values of pressure and velocities typical of blood flow the value of pressure is much greater than the kinetic energy $\frac{1}{2}\bar{u}^2$. This explains why many practitioners in the field use continuity of pressure (instead of total pressure) at the interface without encountering stability problems. This is also true for the interface condition proposed in [35], which does not satisfy the energy inequality (32) a-priori. Indeed, we have performed some numerical studies and found that, for conditions akin to the physiological ones, the results obtained by imposing continuity of pressure, continuity of total pressure or the condition reported in [35] differ less than one percent and do not affect stability.

A physical argument suggests that the total pressure decreases along the flow direction at Γ, as a function of the flow rate. To account for this, one could impose a relation of the type

$$
p_{t,2} = p_{t,1} - \text{sign}(Q)f(Q), \quad \text{at } z = \Gamma,\, t > 0
$$

being f a positive monotone function satisfying $f(0) = 0$. Clearly this condition, coupled with the continuity of Q, satisfies (28). However, the difficulties of finding an appropriate "dissipation function" f for the problem at hand has brought us to consider only the continuity of total pressure, which corresponds to $f \equiv 0$.

3.1 Branching

The arterial and venous systems are characterised by the presence of branching. The flow in a bifurcation is intrinsically three dimensional; yet it may still be represented by means of a 1D model, following a domain decomposition approach, if one is not interested in the flow details. Figure 4 shows a model for a bifurcation. In a first stage we simplify the real geometric structure by imposing that the bifurcation is located exactly on one point and neglecting the effect of the bifurcation angles. This approach has been followed also by other authors, like [16]. An alternative technique is reported in [32], where a separate tract containing the branch is introduced.

In order to solve the three problems in Ω_1 (main branch), Ω_2 and Ω_3 we need to find appropriate interface conditions. The hyperbolic nature of the problem tells us that we need three conditions. The first one states the conservation of mass across the bifurcation, i.e.

$$
Q_1 = Q_2 + Q_3, \quad \text{at } z = \Gamma,\, t > 0. \qquad (36)
$$

We note that the orientation of the axis in the three branches is such that a positive value of Q_i indicates that blood is flowing from the main branch Ω_1 into the other two. By performing an energy analysis similar to that of the previous section on the three branches separately we reach the conclusion that we can obtain a global energy inequality for the coupled problem whenever $p_{t,1}Q_1 - p_{t,2}Q_2 - p_{t,3}Q_3 \geq 0$. If we impose the continuity of total pressure across the bifurcation together with (36) we have $p_{t,1}Q_1 - p_{t,2}Q_2 - p_{t,3}Q_3 = 0$. In this situation it is
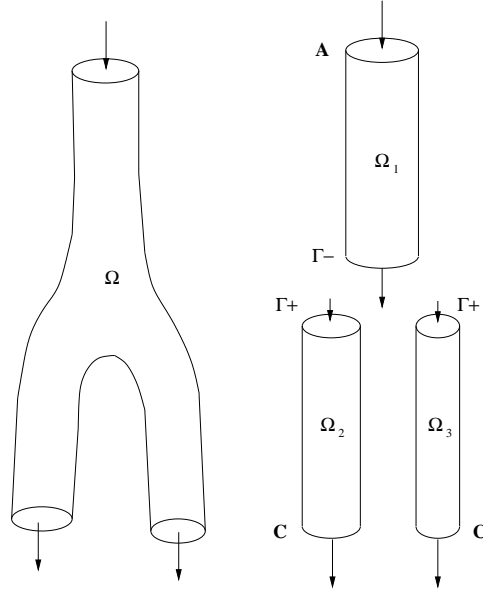
Figure 4: One dimensional model of bifurcation by domain decomposition technique

also expected that the complex flow in the bifurcation will cause a decrease in total pressure in the direction of the flow field across the bifurcation, and this loss should be related to the fluid velocity (or flow rate) and to the bifurcation angles.

A possibility to account for this, derived from the analysis of [12], is to impose, at $z = \Gamma$, that

$$p_{t,1} - \text{sign}(\bar{u}_1) f_1(\bar{u}_1) = p_{t,2} + \text{sign}(\bar{u}_2) f_2(\bar{u}_2, \alpha_2), \tag{37}$$
$$p_{t,1} - \text{sign}(\bar{u}_1) f_1(\bar{u}_1) = p_{t,3} + \text{sign}(\bar{u}_3) f_3(\bar{u}_3, \alpha_3),$$

where α_2 and α_3 are the angles of the branches Ω_2 and Ω_3 with respect to the main one (see fig. 5); f_1, f_2 and f_3 are positive functions and equal to zero when the first argument is zero. These can be chosen to be:

$$f_1(u) = \gamma_1 u^2, \quad f_i(u, \alpha) = \gamma_i u^2 \sqrt{2(1 - \cos \alpha)}, \; i = 2, 3, \tag{38}$$

where the γ_i are positive coefficients.

In the numerical scheme, (36) and (37) will be complemented by three compatibility relations, which can be expressed again by the extrapolation of the outgoing characteristic variables. We have thus a non linear system for the six unknowns $A_i^{n+1}, Q_i^{n+1}, i = 1, 2, 3$, at the interface location Γ, which is solved by a Newton iteration.

Some numerical tests have been made to investigate the effect of the bifurcation angles using relations (37) and (38) ($\gamma_1 = 0$, γ_2 and $\gamma_3 = 2$). The length of the three domains has been taken equal to $10 \; cm$. The following parameters have been chosen: $E = 3 \; 10^6 \; dyne/cm^2$, $h_0 = 0.05 \; cm$, $R_0 = 0.5 \; cm$, $\rho = 1 \; gr/cm^3$, $\alpha = 1$, $\nu = 0.035 \; cm^2/s$, equal in all three vessels. At the inlet of Ω_1 we have imposed a half sine input pressure wave of period $0.1 \; s$ and amplitude $20000 \; dyne/cm^2$, while a non-reflecting condition has been imposed at the outlet sections of Ω_2 and Ω_3. In Figures 6, 7 and 8 we show the time variation of the area A and the two characteristic variables W_1 and W_2 at a location placed at the midpoint of Ω_1, Ω_2 and Ω_3, respectively, for different values of α_1 and α_2. In particular, $\alpha_1 = \alpha_2 = 0$ corresponds to the case where we impose just the continuity of the total pressure, ignoring the dissipative effects caused by the kinks. We may note that accounting for the angles increase the amplitude of the wave reflected by the bifurcation (increase in the amplitude of W_2 in Fig 6), with also an increase of area and, consequently, the pressure level in Ω_1. On the contrary, there is a reduction in the strength of the wave transmitted into Ω_2 and Ω_3 (as expected). The result of this simple experiment shows that indeed the dissipation caused by the flow deviation at bifurcations could be relevant.

Also in this case, due to the difficulty of finding suitable values of the "dissipation functions" f for the problem at hand, we have preferred to put them to zero and impose the continuity of the total pressure across the bifurcation,
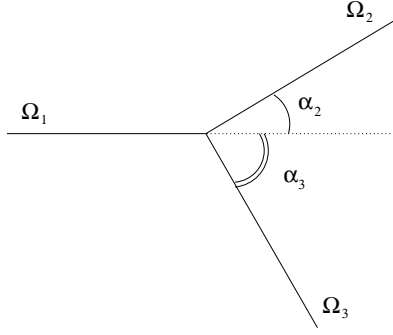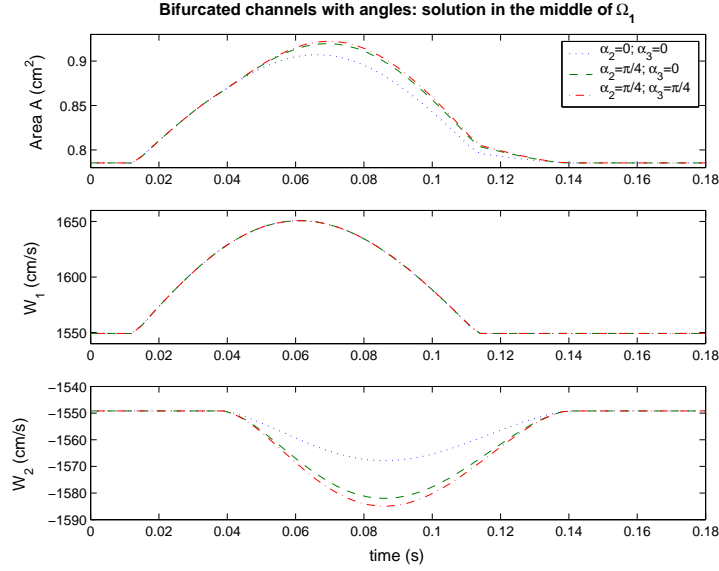
Figure 5: A sketch of a branching.

Figure 6: Solution dependence on bifurcation angles: area and characteristic variables at the middle point of domain Ω_1 are reported.

i.e.,

$$p_{t,1} = p_{t,2} = p_{t,3}, \quad \text{at } z = \Gamma. \tag{39}$$

Thence, in the remaining part of this work we will neglect this effect.

3.2 Bifurcated channel with endograft

Here we show an application of the one dimensional model to a real-life problem. Abdominal aortic aneurysms (AAA) represent a significant and relatively common vascular problem. They are characterised by an abnormal dilatation of a portion of the aorta. This swollen region would enlarge with time and, without a surgical treatment, it will eventually break with fatal consequences. Even if open surgical repair is still the standard treatment for AAA, endografts and endovascular stent grafts begin to play a major role as they allow a less invasive treatment (fig. 9).

The presence of an endograft may be treated by our one-dimensional model as a bifurcated channel with varying mechanical properties, as shown in Fig. 10. The domain is decomposed into 6 regions, Ω_i, $i = 1, \ldots, 6$ and the interface conditions of type (33) or (36)-(39) are used where appropriate.
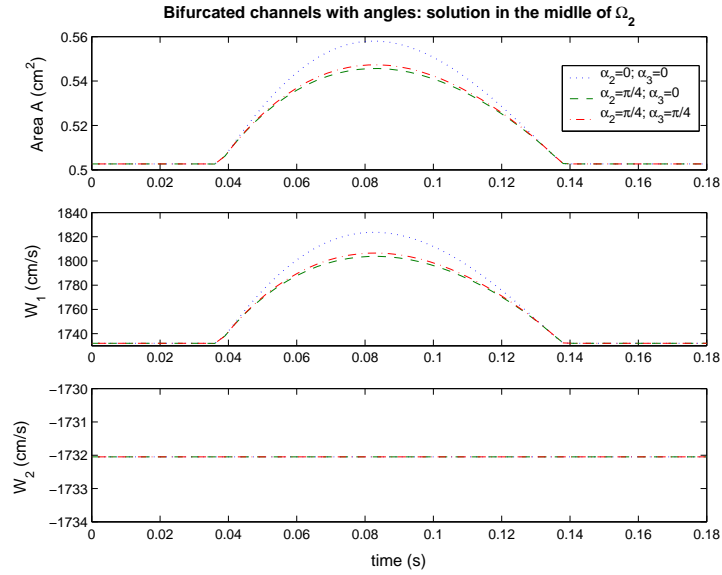
Figure 7: Solution dependence on bifurcation angles: area and characteristic variables at the middle point of domain Ω_2 are reported.
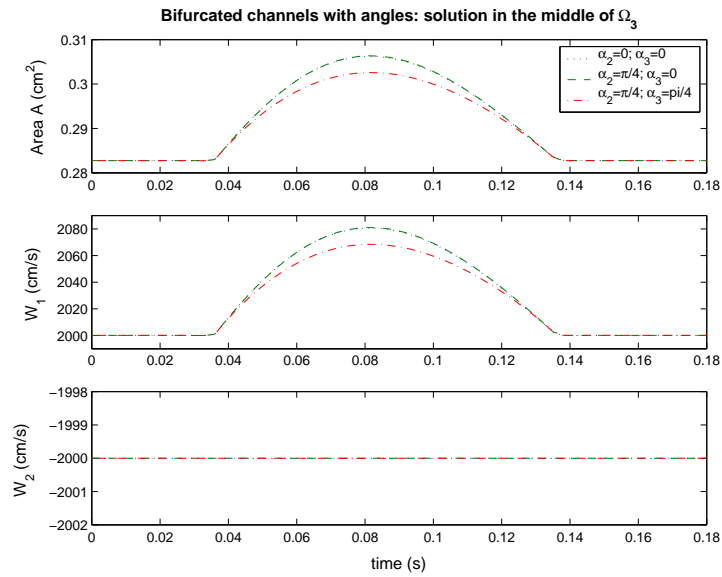

Figure 8: Solution dependence on bifurcation angles: area and characteristic variables at the middle point of domain Ω_3 are reported.

Figure 9: Endograft placement in the surgical treatment of abdominal aortic aneurysms.

A preliminary numerical test has been carried out by selecting all Ω_i to be of equal length L=5 cm. We considered everywhere $\rho = 1$ gr/cm^3, $\nu = 0.035$ cm^2/s, $\alpha = 1$, $h_0 = 0.05$ cm; while the Young's moduli have been taken to be equal to $E_{endograft} = 60 \ 10^6$ $dyne/cm^2$ for the endografted part (Ω_i, $i = 2, 3, 5$) and $E_{vessel} = 10 \ 10^6$ $dyne/cm^2$ for the remaining subdomains. The vessel reference radii have been taken to be $R_{0,1} = R_{0,2} = 0.6$ cm, $R_{0,3} = R_{0,4} = 0.4$ cm and $R_{0,5} = R_{0,6} = 0.5$ cm.

At inlet we have imposed a half sine pressure wave of period 0.1 s and amplitude 20000 $dyne/cm^2$.
The spatial grid was uniform with a total of 546 nodes. The computations were carried out with a time step Δt 0.00001 s.

Figures 11, 12, 13 report the time evolution for the area A and the two characteristic variables W_1 and W_2 at three given points, respectively at the middle of Ω_1, and of Ω_2 and of Ω_6. By inspecting figure 11 we remark that in W_1 we find the input wave imposed at inlet, while in W_2 we find the composition of two effects, the wave reflected from the beginning of the endograft and the wave reflected from the branching point. These modify the sinusoidal shape of the area A. On Figure 12 we find in W_2 only the wave reflected from the branching point. Finally, in figure 13 we do not find reflected waves (being the outlet boundary condition an absorbing one); moreover, in W_1 we can observe the part of the wave passing through the branches.

4 More complex wall models

The mechanical model used to describe the vessel wall dynamics was based on the assumption of an instanta-neously elastic equilibrium, according to which the vessel wall responds to a change in the fluid pressure by adapting its section area, following a perfectly elastic law.

In reality, the mechanical behaviour of arterial wall is much more complex (see e.g. [13]). Although it is arguable whether there is a need for a sophisticated mechanical modelling when so many simplifications have already been made both at the geometrical and at fluid-dynamics level, improving the structural description may serve several purposes:

- to study the overall effects on the flow field of the different physical terms that might be included, such as wall inertia, viscoelasticity, pre-stress state;
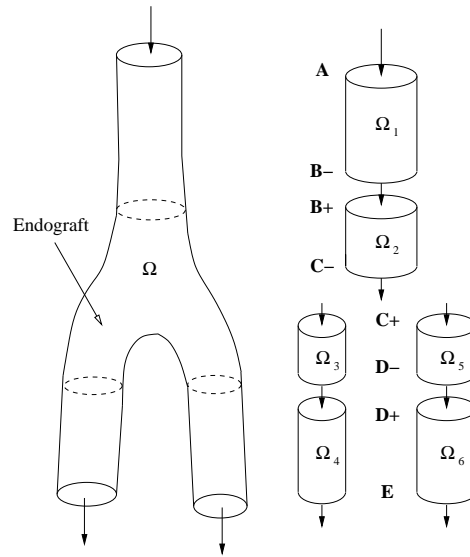
15

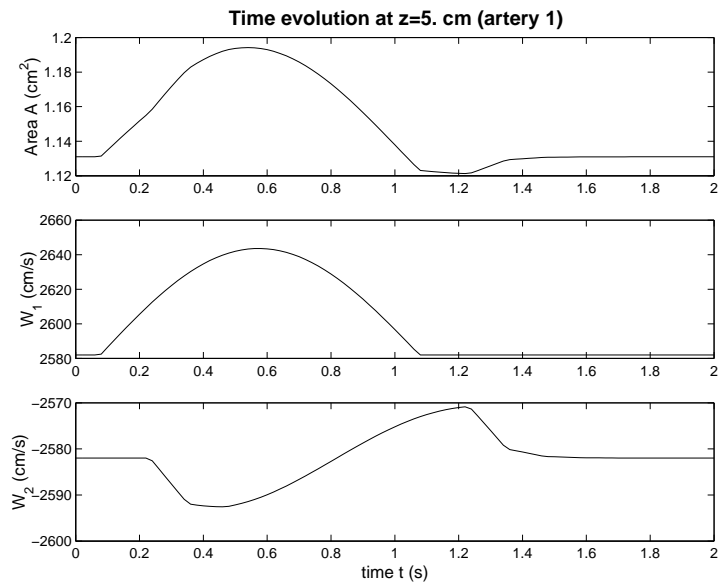Figure 10: Modelling (left) and domain decomposition (right) of a bifurcation with an endograft.

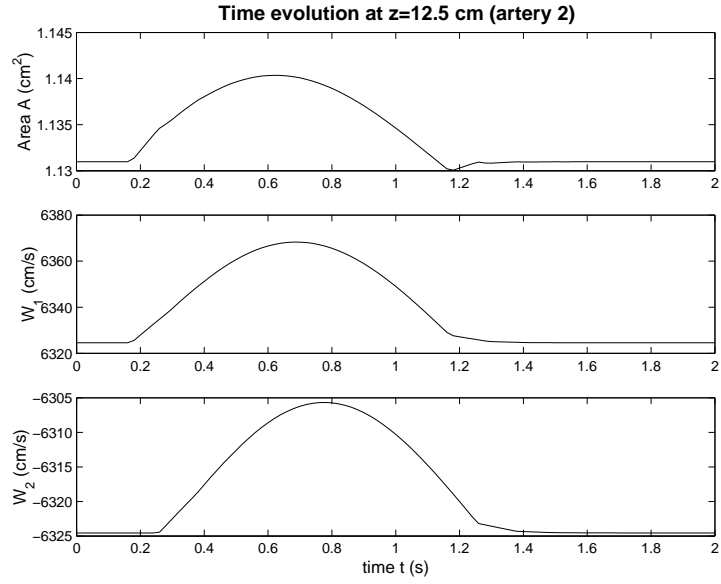Figure 11: Bifurcation with endograft: time evolution for the area and the characteristic variables in the middle of domain Ω_1.

16

Figure 12: Bifurcation with endograft: time evolution for the area and the characteristic variables in the middle of domain Ω_2.
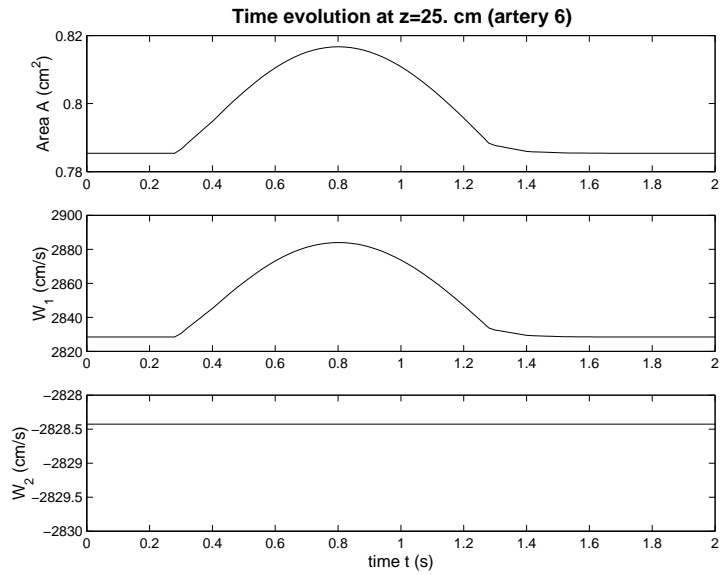

Figure 13: Bifurcation with endograft: time evolution for the area and the characteristic variables in the middle of domain Ω_6.

- to verify the relevance of these terms for the problem at hand on the basis of realistic physiological or pathological values of the various coefficients.

The structural model will be obtained from the general equilibrium laws by imposing geometrical simplifications consistent with those used to derive the flow equations. In particular, we still consider displacements η in the radial direction only. This is a reasonable assumption since some recent results ([21]) using membrane models for the wall structure which account for the effects of transversal displacements show that these are negligible.

The differential equation we will consider is in fact the generalised string model (5), where we neglect the second viscoelastic term, i.e $\tilde{c} = 0$. To obtain an equation of the form $A = A_0 + \pi\eta^2$, we linearise the time derivatives, following [9], as follows

$$\frac{\partial \eta}{\partial t} \simeq \frac{1}{2\sqrt{A_0}\sqrt{\pi}}\frac{\partial A}{\partial t} \tag{40}$$

$$\frac{\partial^2 \eta}{\partial t^2} = \frac{1}{\sqrt{\pi}}\frac{\partial^2}{\partial t^2}\left(\sqrt{A} - \sqrt{A_0}\right) \simeq \frac{1}{2\sqrt{\pi A_0}}\frac{\partial^2 A}{\partial t^2}. \tag{41}$$

Therefore, the adopted model may be written as

$$m\frac{\partial^2 A}{\partial t^2} - \gamma\frac{\partial A}{\partial t} - a\frac{\partial^2}{\partial z^2}(\sqrt{A} - \sqrt{A_0}) + \beta\frac{\sqrt{A} - \sqrt{A_0}}{A_0} = P, \tag{42}$$

where we have taken, as before, $P_{ext} = 0$ and

$$m = \frac{\rho_w h_0}{2\sqrt{\pi}\sqrt{A_0}}, \quad \gamma = \frac{\tilde{\gamma}}{2\sqrt{\pi}\sqrt{A_0}}, \quad a = \frac{\tilde{a}}{\sqrt{\pi}},$$

while β is still given by (10).

This model should be integrated with the fluid equations (2) and (3). The objective is to retain the basic two-equations structure of the model. Furthermore, we will assume that the additional terms are of less importance than the basic elastic response function $\beta\frac{\sqrt{A} - \sqrt{A_0}}{A_0}$ considered in the derivation of the previous model. This assumption permits the use of an operator splitting procedure for the numerical approximation.

The coupling between (2, 3) and (42) is through the pressure term $\frac{A}{\rho}\frac{\partial}{\partial z}(P - P_{ext})$ in the momentum equation. Therefore, the continuity equation (2) will remain unaltered and, following [9], we will use it to replace the time derivatives of A with the space derivative of Q.

We are mainly interested in identifying the effects of the extra terms on the vessel mechanics. The next sections will systematically analyse the effect of each of the added in turn.

4.1   Wall inertia term

The inertia term accounts for the wall mass and its acceleration: using physical arguments we can argue that it will be important only in case of large vessel mass and/or high frequency wave (big acceleration). In these cases we expect oscillations to occur at a frequency dependent on the wave length.

The contribution of this term in the momentum equation can be written, using the continuity equation, as

$$\frac{A}{\rho}\frac{\partial}{\partial z}\left(m\frac{\partial^2 A}{\partial t^2}\right) = -\frac{Am}{\rho}\frac{\partial^3 Q}{\partial t \partial z^2}. \tag{43}$$

System (13), augmented by the inertia term would then read

$$\begin{cases} \dfrac{\partial A}{\partial t} + \dfrac{\partial Q}{\partial z} = 0 \\[2mm] \dfrac{\partial Q}{\partial t} + \dfrac{\partial}{\partial z}F_2(A, Q) - \dfrac{Am}{\rho}\dfrac{\partial^3 Q}{\partial t \partial z^2} = B_2(A, Q), \end{cases} \tag{44}$$

where $F_2(A, Q)$ and $B_2(A, Q)$ denote the second component of the flux $\mathbf{F}$ and of the source term $\mathbf{B}$, respectively.

The differential system (44) may be written in an equivalent way by splitting the flow rate $Q = \widehat{Q} + \widetilde{Q}$, where $\widehat{Q}$ and $\widetilde{Q}$ are implicitly defined through the set of equations

$$\frac{\partial A}{\partial t} + \frac{\partial Q}{\partial z} = 0$$

$$\frac{\partial \widehat{Q}}{\partial t} + \frac{\partial}{\partial z} F_2(A, Q) = S(A, Q) \tag{45}$$

$$\frac{\partial \widetilde{Q}}{\partial t} - \frac{Am}{\rho} \frac{\partial^3 Q}{\partial t \partial z^2} = 0.$$

This allows us to devise the following operator splitting strategy. On each time interval $[t^n, t^{n+1}]$, $n \geq 0$, system $(45)_{1,2}$ by the Taylor-Galerkin scheme described in Sec. 2.2 and we correct the mass flux by employing Eq. $(45)_3$. More precisely, the adopted finite element formulation for the latter equation reads: given A_h^{n+1} and $\widehat{Q}_h^{n+1}$, find $\widetilde{Q}_h \in V_h^0$ such that

$$\left(\frac{1}{A_h^{n+1}} \widetilde{Q}_h^{n+1}, \psi_h \right) + \frac{m}{\rho} \left(\frac{\partial \widetilde{Q}_h^{n+1}}{\partial z}, \frac{\partial \psi_h}{\partial z} \right) = \frac{m}{\rho} \left(\frac{\partial \widehat{Q}_h^{n+1}}{\partial z}, \frac{\partial \psi_h}{\partial z} \right), \quad \forall \psi_h \in V_h^0.$$

This corresponds to having imposed a homogeneous boundary condition for the correction term $\widetilde{Q}$.
An alternative approach can be found in [1].

In the following numerical experiments we have set $\rho = 1 \, gr/cm^3$, $\nu = 0.035 \, m^2/s$, R_0 has been taken constant and equal to 0.5 cm, $h_0 = 0.05 \, cm$ and $E = 3 \, 10^6 \, dyne/cm^2$. The simulations have been carried out using a time step $\Delta t = 1 \, 10^{-5} \, s$.
Figure 14 shows the results for a realistic test problem where the vessel wall density is set to $\rho_w = 1 gr/cm^3$ and we take a wave of length 32 cm (picture on the top-left of Figure 14). It may be noted that the inertia term yields a relative variation in the vessel area of the order of 10^{-3}. We may also note the high frequency oscillations induced by the inertia term. Clearly, in real conditions these oscillations are damped out by the viscoelastic term. As high frequency are solicited, the variation in the flow rate behaviour is more important. We also report some numerical experiments carried out in the same geometrical configuration using a pressure wave pulse of length 4. cm (pictures on the top-left of Figures 15 and 16) and a wall density of 1 and 100 gr/cm^3, respectively. These tests have been carried out to enhance the inertia effects and are reported in Figures 15 and 16. Note, in particular, that the value 100 gr/cm^3 is unrealistic in physiological conditions. These tests show that the inertia term play a major role when the mass or the vessel acceleration are important.
A qualitative comparison with the result obtained by a two dimensional fluid-structure interaction code has been carried out only for the test case of Figure 15; a good agreement has been found.

4.2 Viscoelastic term

In the generalised string model there are two possible viscous effects. Here, we have considered only the term in the form $\tilde{\gamma} \frac{\partial \eta}{\partial t}$, since the term $(\tilde{c} \frac{\partial^3 \eta}{\partial t \partial z^2})$ will produce a fourth order spatial derivative in the momentum equation that makes its numerical treatment more difficult.

After introducing the term in the momentum equation and using the continuity equation, the modified system reads

$$\begin{cases} \dfrac{\partial A}{\partial t} + \dfrac{\partial Q}{\partial z} = 0 \\[2mm] \dfrac{\partial Q}{\partial t} + \dfrac{\partial F_2(A, Q)}{\partial z} - \dfrac{A\gamma}{\rho} \dfrac{\partial^2 Q}{\partial z^2} = B_2(A, Q). \end{cases} \tag{46}$$

This system has been solve by an operator splitting procedure similar to that introduced before and an implicit Euler discretisation for the correction term $\widetilde{Q}$.
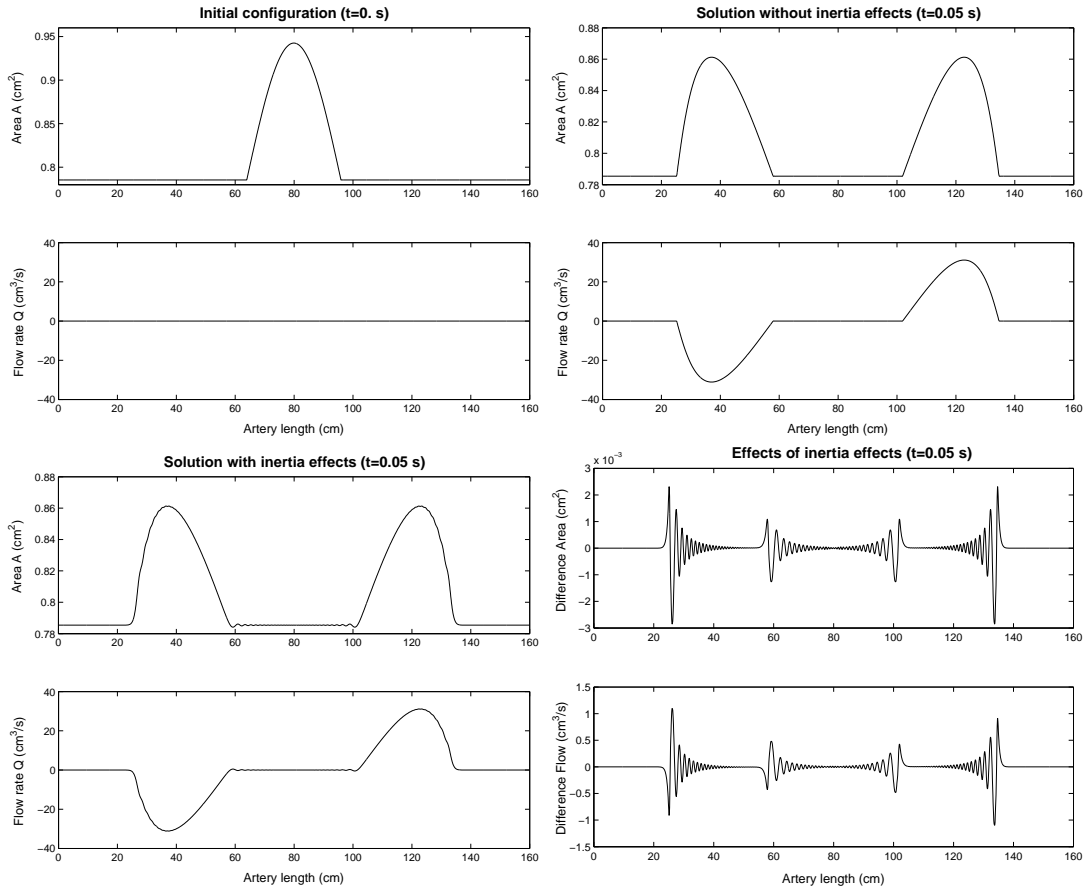
Figure 14: Inertia effects on the solution; on the top-left the initial configuration is reported: a half sine wave of length 35 cm. The solutions without inertia term (top-right), with inertia term (bottom-left) and the difference between the two (bottom-right) for a fixed time (0.05 s) are reported too.
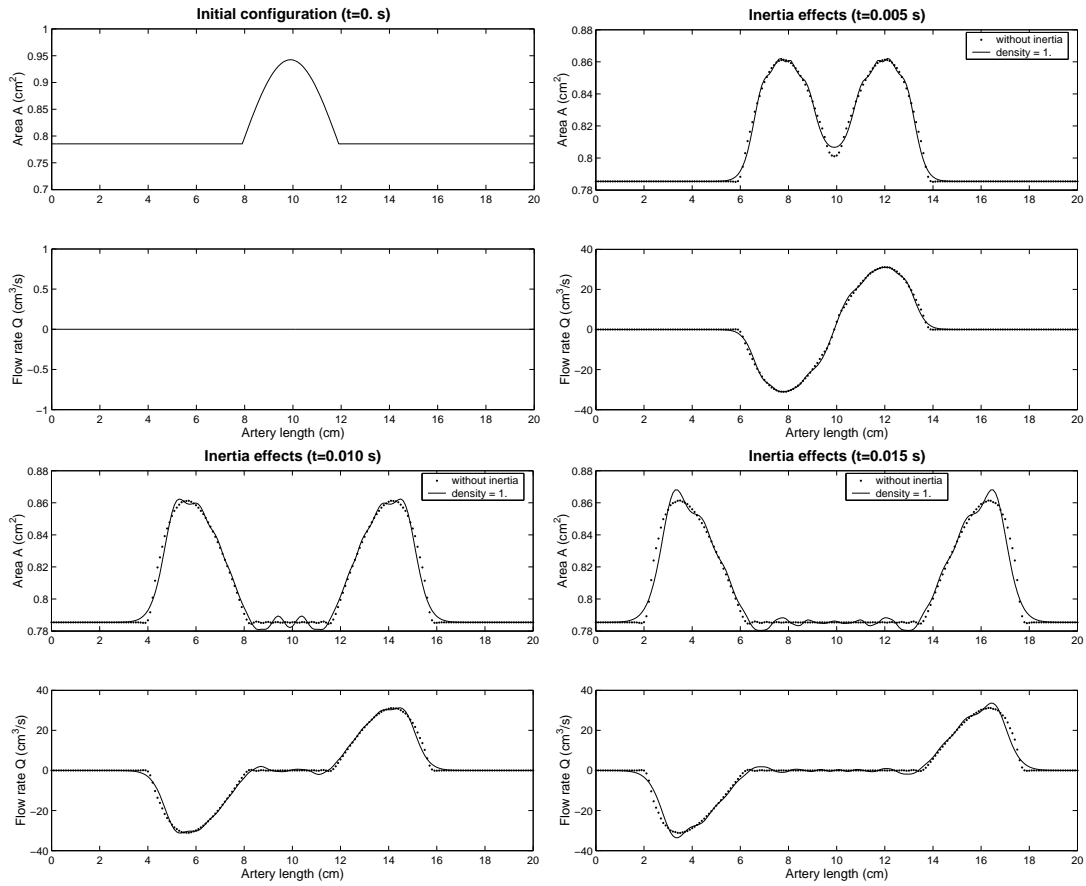
Figure 15: Inertia effects on the solution; on the top-left the initial configuration is reported: a half sine wave of length 4 cm. The solutions without inertia term (dotted line) and with inertia term, wall density set to 1 gr/cm^3, (continuous line) for different time steps are also reported.
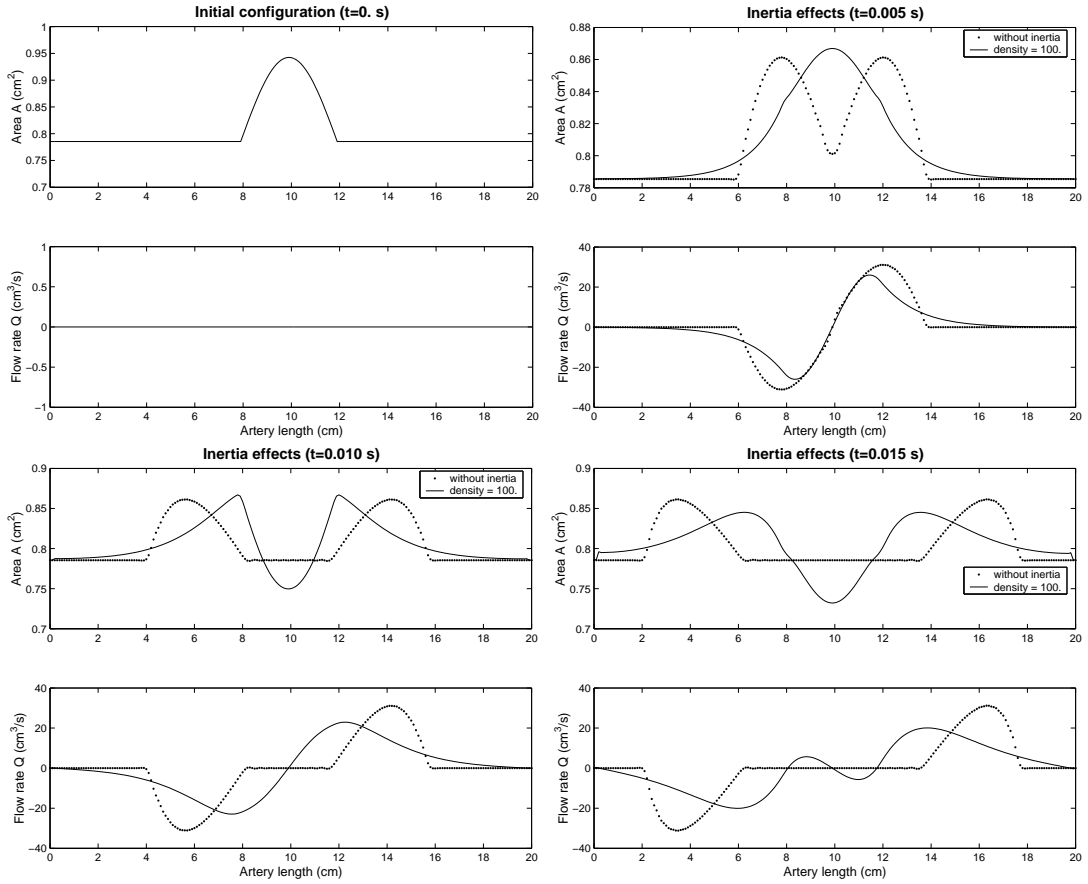
21

Figure 16: Inertia effects on the solution; on the top-left the initial configuration is reported: a half sine wave of length 4 cm. The solutions without inertia term (dotted line) and with inertia term, wall density set to 100 gr/cm^3, (continuous line) for different time steps are also reported.
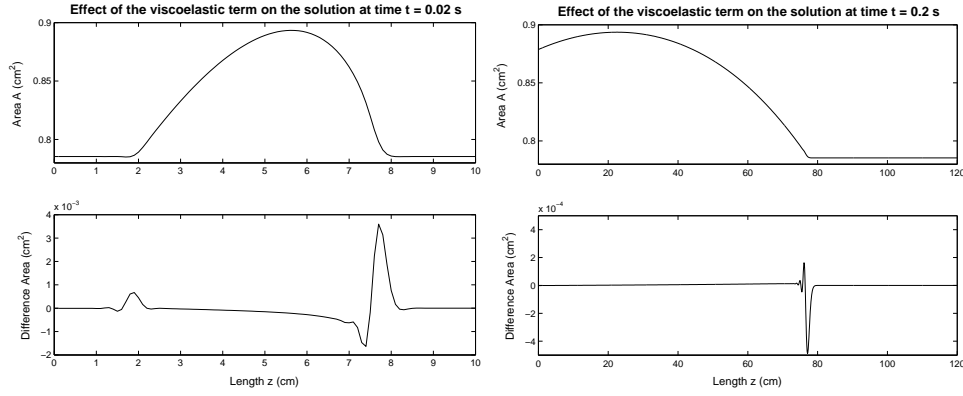
Figure 17: Viscoelasticity effects on the solution at two given time steps: solution of the problem without viscoelasticity term (top) and difference between the solutions with and without viscoelastic term (bottom).

Tests have been carried out to investigate the effects of the viscoelastic term. We set $\rho = 1 \ gr/cm^3$, $\nu = 0.035$ m^2/s, $R_0 = 0.5 \ cm$, $h_0 = 0.05 \ cm$ and $E = 3 \ 10^6 \ dyne/cm^2$. The simulations have been carried out with a time step $\Delta t = 1 \ 10^{-4} \ s$ and a space discretization $\Delta x = 0.1 \ cm$.

In Figure 17 we report the results of a short half sine pressure wave (period 0.015 s, amplitude 20000 $dyne/cm^2$) and a longer one (period 0.3 s, amplitude 20000 $dyne/cm^2$) imposed at inlet. We should note that the solutions with ($\gamma = 3 \ gr/cm^3 s$) and without the viscoelastic term have a relative difference in the area of less than 1 %.

4.3 Longitudinal elasticity term

Experimental findings show that vessel walls are longitudinally pre-stressed [10]. This originates the second z derivative term in the generalised string model [24]. Accounting for this term by using the techniques previously illustrated would produce a modified system of the type

$$\begin{cases} \dfrac{\partial A}{\partial t} + \dfrac{\partial Q}{\partial z} = 0 \\[2mm] \dfrac{\partial Q}{\partial t} + \dfrac{\partial F_2(A,Q)}{\partial z} - \dfrac{Aa}{\rho}\dfrac{\partial^3}{\partial z^3}\left(\sqrt{A} - \sqrt{A_0}\right) = B_2(A,Q). \end{cases} \tag{47}$$

Solving this system by an operator splitting technique like that presented in Sec. 4.1 would require the solution of a differential equation for the correction term $\widetilde{Q}$ given by

$$\frac{\partial \widetilde{Q}}{\partial t} - \frac{Aa}{\rho}\frac{\partial^3}{\partial z^3}\left(\sqrt{A} - \sqrt{A_0}\right) = 0. \tag{48}$$

The correction $\widetilde{Q}_h^{n+1} \in V_h^0$ has been computed by a collocation procedure and using a finite difference approximation for the third derivative term of A_h^{n+1} (which is computed in the first step of the operator splitting procedure).

The effect of the longitudinal pre-stress is more important when strong area gradients are present. To analyse thus, we considered a stented artery of total length $L = 15 \ cm$ with a stent of length 5 cm placed in the middle. The vessel has a radius $R_0 = 0.5 \ cm$ and $h_0 = 0.05 \ cm$. The Young's modulus is $E = 3 \ 10^6 \ dyne/cm^2$ for the healthy portion of the artery and $E_s = 30 \ 10^6 \ dyne/cm^2$ for the stented part. At $z = 5 \ cm$ and $z = 10 \ cm$ the Young's modulus has been regularised by a fifth-order function (as done in [8]); the length of the variation zone was 0.1 cm. The coefficient $\tilde{a}$ was set to $10^4 \ gr/s^2$. Finally, we have taken $\rho = 1 \ gr/cm^3$, $\nu = 0.035 \ cm^2/s$ and $\alpha = 1$.

At inlet we imposed a half sine pressure wave of period $T = 0.4 \ s$ and amplitude of 20000 $dyne/cm^2$.
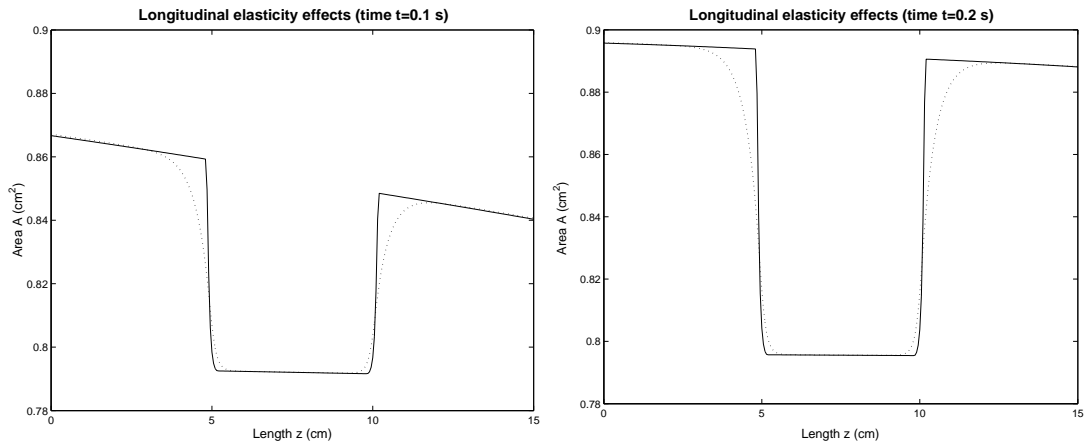
Figure 18: Longitudinal elasticity effects on the solution at two different time steps (the dotted line represents the solution with the longitudinal pre-stress term).

Figure 18 shows that, without the longitudinal elasticity term (solution represented by a continuous line), there is an abrupt variation in the area. Clearly this solution is not physiological as we cannot have, in the limit, a discontinuous area. Taking in account the effect of the longitudinal elasticity term, that "discontinuity" is smoothed with a jump between the values of the area on the left and the right of the same magnitude.

5   Conclusions

In the numerical simulation of blood flow one dimensional models may play an important role, in particular when one is not interested in the details of the flow field but just to the evolution of averaged quantities along the arterial tree. To that respect, they allow a good description of pressure waves propagation in arteries at a reasonable computational cost. The wave propagation phenomenon is due to the fluid-structure interaction. The description of the mechanical behaviour of the vessel wall thus plays a fundamental role.

We have here considered how the model may be modified to account for different terms in the mechanical relation, yet with the aim of maintaining a simple two-equation structure.

We have analysed these terms in turn and we reached the conclusion that for physiological values of pressure and flow velocity they are not particularly relevant, thus the use of the simpler model based on an algebraic relation between pressure and section area is justified. They however may have a more marked effect when, in pathological situations or because of the implant of a prosthesis, there are strong gradients in the solution. In particular, longitudinal pre-stress has an important regularising effect.

However, the case of a prosthesis implant may also be tackled by using a domain decomposition approach. We have shown how the continuity of total pressure is a sound interface condition in this case, together with the continuity of the mass flux.

A domain decomposition approach is also necessary for the treatment of branching. Here again the continuity of total pressure guarantee a mathematically sound coupling. Bifurcation angle may also be accounted for with empirical relations.

A natural continuation of this work is the simulation of the global cardiovascular system. This task will be accomplished by coupling a network of one dimensional models for the arterial tree with lumped parameter models describing the action of heart, the capillary bed, the venous system and the pulmonary circulation.

24

References

[1] D. Ambrosi and L. Quartapelle. A Taylor-Galerkin method for simulating nonlinear dispersive water waves. *J. Comput. Phys.*, 146(2):546–569, 1998.

[2] K. Boukir, Y. Maday, and B. Métivet. A high order characteristics method for the incompressible Navier-Stokes equations. *Comput. Methods Appl. Mech. Engrg.*, 116(1-4):211–218, 1994. ICOSAHOM'92 (Montpellier, 1992).

[3] J. Donea, S. Giuliani, H. Laval, and L. Quartapelle. Time-accurate solutions of advection-diffusion problems by finite elements. *Comp. Meth. Appl. Mech. Engng.*, 45:123–145, 1984.

[4] F. Dubois and P. Le Floch. Boundary conditions for nonlinear hyperbolic systems of conservation laws. *Journal of Differential Equations*, 71:93–122, 1988.

[5] E. Finzi. Résolution d'écoulements sanguins avec une technique multigrille/multimodèles. Travail de fin d'études, Ecole normale Supérieure de Techniques Avancées, Paris, Septembre 2001.

[6] L. Formaggia, J.-F. Gerbeau, F. Nobile, and A. Quarteroni. On the coupling of 3D and 1D Navier-Stokes equations for flow problems in compliant vessels. *Comp. Methods in Appl. Mech. Engng.*, 191:561–582, 2001.

[7] L. Formaggia, F. Nobile, J.-F. Gerbeau, and A. Quarteroni. Numerical treatment of defective boundary conditions for the Navier-Stokes equations. *SIAM J. Num. An.*, 40, 1:376–401, 2002.

[8] L. Formaggia, F. Nobile, and A. Quarteroni. A one dimensional model for blood flow: application to vascular prosthesis. In I. Babuska, T. Miyoshi, and P.G. Ciarlet, editors, *Mathematical Modeling and Numerical Simulation in Continuum Mechanics*, volume 19 of *Lecture Notes in Computational Science and Engineering*, pages 137–153, Berlin, 2002. Springer-Verlag.

[9] L. Formaggia, F. Nobile, A. Quarteroni, and A. Veneziani. Multiscale modelling of the circulatory system: a preliminary analysis. *Computing and Visualisation in Science*, 2:75–83, 1999.

[10] Y.C. Fung. *Biomechanics: Mechanical Properties of Living Tissues.* Springer-Verlag, New York, 1993.

[11] E. Godlewski and P.-A. Raviart. *Numerical Approximation of Hyperbolic Systems of Conservation Laws*, volume 118 of *Applied Mathematical Sciences*. Springer, New York, 1996.

[12] H. Holden and N.H. Risebro. Riemann problems with a kink. *SIAM J. Math. Anal.*, 30,3:497–515, 1999.

[13] G.A. Holzapfel, T.C. Gasser, and R.W. Ogden. A new constitutive framework for arterial wall mechanics and a comparative study of material models. *Journal of Elasticity*, 61:1–48, 2000.

[14] M. Olufsen. A one-dimensional fluid dynamic model of the systemic arteries. In J. Ottesen and M. Danielsen, editors, *Proceedings from Mathematical Modelling in Medicine, September 1997, Roskilde University*. Roskilde University Press, 1997.

[15] M. Olufsen. *Modeling the arterial system with reference to an anestesia simulator*. PhD thesis, Rotskilde Univ., 1998. Tekst 345.

[16] M. Olufsen and J. Ottesen. A fluid dynamical model of the aorta with bifurcations. Tekst 297, Rotskilde Univ., 1995.

[17] T.J. Pedley. *The Fluid Mechanics of Large Blood Vessels*. Cambridge University Press, Cambridge, G.B., 1980.

[18] C.S. Peskin. *Partial Differential Equations in Biology*. Courant Institute of Mathematical Sciences, New York University, USA, 1976.

[19] F. Phythoud, N. Stergiopulos, and J.-J. Meister. Forward and backward waves in the arterial system: nonlinear separation using Riemann invariants. *Technology and Health Care*, 3:201–207, 1995.

[20] R. Pietrabissa, A. Quarteroni, G. Dubini, A. Veneziani, F. Migliavacca, and S. Ragni. From the global cardiovascular hemodynamics down to the local blood motion: preliminary applications of a multiscale approach. In E. Onate et al., editor, *ECCOMAS 2000*, Barcelona, 2000.

[21] G. Pontrelli. A mathematical model of flow through a viscoelastic tube. *Meccanica*, 2001.

[22] G. Pontrelli and E. Rossoni. Modelling the fluid-wall interaction in a blood vessel. Quad. IAC/CNR 35/2000, submitted, 2000.

[23] L. Quartapelle. *Numerical solution of the incompressible Navier-Stokes equations*. Birkhäuser Verlag, Basel, 1993.

[24] A. Quarteroni and L. Formaggia. *Modelling of Living Systems*, chapter Mathematical Modelling and Numerical Simulation of the Cardiovascular System. Handbook of Numerical Analysis. Elsevier Science, Amsterdam, 2002. submitted.

[25] A. Quarteroni, M. Tuveri, and A. Veneziani. Computational vascular fluid dynamics: Problems, models and methods. *Computing and Visualisation in Science*, 2:163–197, 2000.

[26] A. Quarteroni and A. Valli. *Numerical Approximation of Partial Differential Equations*. Springer-Verlag, Berlin, 1994.

[27] A. Quarteroni and A. Valli. *Domain Decomposition Methods for Partial Differential Equations*. The Clarendon Press Oxford University Press, New York, 1999. Oxford Science Publications.

[28] V. Rideout and D. Dick. Difference-differential equations for fluid flow in distensible tubes. *IEEE Trans. Biomed. Eng.*, BME-14(3):171–177, 1967.

[29] S.J. Sherwin, L. Formaggia, and J. Peiró. Computational modelling of 1D blood flow with variable mechanical properties. In *Proceedings of ECCOMAS CFD 2001*, ECCOMAS, September 2001. CD-ROM Edition.

[30] S.J. Sherwin, L. Formaggia, J. Peiró, and V. Franke. Computational modelling of 1D blood flow with variable mechanical properties and its application to the simulation of wave propagation in the human arterial system. *Int. J. Numer. Meth. Fluids*, 2002.

[31] N.P. Smith, A.J. Pullan, and P.J. Hunter. An anatomically based model of coronary blood flow and myocardial mechanics. *SIAM J. Appl. Math.*, 2002. (to appear).

[32] J.C. Stettler, P. Niederer, and M. Anliker. Theoretical analysis of arterial hemodynamics including the influence of bifurcations, part i: Mathematical model and prediction of normal pulse patterns. *Annals of Biomedical Engineering*, 9:145–164, 1981.

[33] V.L. Streeter, W.F. Keitzer, and D.F. Bohr. Pulsatile pressure and flow through distensible vessels. *Circulation Research*, 13:3, 1963.

[34] K.W. Thompson. Time dependent boundary conditions for hyperbolic systems. *J. Comp. Physics*, 68:1–24, 1987.

[35] S. Čanić. Blood flow through compliant vessels after endovascular repair: wall deformations induced by the discontinuous wall properties. *Computing and Visualisation in Science*, 4, 3:147–155, 2002.

[36] N. Westerhof, F. Bosman, C. Vries, and A. Noordergraaf. Analog studies of the human systemic arterial tree. *J. of Biomech*, 2:121–143, 1969.